ON THE SIMULATION OF A MONO-ACTUATOR BI-AXIAL AZIMUTH PV SYSTEM

M. VĂTĂŞESCU[1]   D.V. DIACONESCU[1]   I. VIŞA[1]

Abstract: *The current trends in solar tracking systems and their appropriate tracking programs aim to capture the most of the solar radiation using simple devices. These have to be done considering the specific local and climatic configuration of the implementation area. In order to accomplish these conditions, the present paper proposes a non-adjustable mono-actuator, bi-axial azimuth mechanism, starting from a previous adjustable proposal, and determines its optimised length dimensions for Braşov's climatic conditions, by means of numerical simulations. Consequently, the received direct solar radiation amount is estimated considering the clouds' presence in the sky during each month by means of a specific factor referred to as the Clouds' Crossing Factor.*

Key words: *direct solar radiation, PV module, Azimuth Tracking System, Clouds' Crossing Factor.*

1. Introduction

Solar radiation is the only inexhaustible, constant, environmentally-friendly and over-sufficient source of energy for mankind. It is valued due to its warming effect and to its potential to be converted into electrical energy. In order to generate an electrical effect, the solar radiation has to be captured only on a normal solar absorbing surface [1], [7], [8]. The aim of gaining an ever-increasing amount of solar energy based on cheaper and more effective devices has channelled research into new types of bi-axial tracking systems. Representative for this category are bi-axial azimuth systems which track a PV platform using a single rotational actuator and a spatial tracking linkage. This sub-category can be exemplified by two international published solutions presented in Figures 1a and b.

The first solution is a Greek patent proposal (see Figure 1a) [4] which contains a planar linkage 3-8-4-1-3 of type PRRR (P = prismatic joint; R = revolute joint) and a spatial cam gear (9-3-8-9); by means of a fixed cylindrical cam 9, the spatial cam gear converts the azimuth movement of the shaft 3 into a vertical translation movement of a fellow 8 that achieves the elevation movement of the PV platform 1, by means of two bars 4. Thus, owing to this compound tracking mechanism, the PV elevation angular displacement is obtained from the azimuth movement of the shaft 3 (driven by the actuator 10). The main inconveniences of this solution consist of its high complexity and its non-congruent contacts of the fellow 8.

The second solution is a Spanish patent proposal shown in Figure 1b [5]. This

---

[1] Centre "Advanced Research on Mechatronics", *Transilvania* University of Braşov.

solution consists of a spatial linkage 1-2-4-8-1 of type RRHH (H = Hook joint); by means of this spatial linkage, the PV elevation angular movement is obtained from the azimuth movement of the head 2 (driven by a slew actuator).

The linkage is fitted with two adjustable screw devices that allow PV system adjustment to the climatic features: the device 7, which adjusts the inferior H-joint position (i.e. the distance between the 8-1 H-joint and axis of the 1-2 R-joint) and the device 9, which adjusts the length of the bar 8 (i.e. the distance between the two H-joints). Although this tracking linkage is relatively simple, the two adjustable screw devices both increase its complexity and reduce its stiffness. Neither of the above-mentioned solutions (see Figures 1a and b)

provides any data regarding the optimal dimensional correlations of the linkages; also, no data are supplied on a main working parameter: the pressure angle at the joint between the PV frame and the swing bar.

According to Figure 2a, a new improved variant of RRSS type (S = spherical joint) has been derived from the previous solution (see Figure 1b); this spatial tracking linkage was modelled and analyzed in paper [3]. In contrast with the solution in Figure 1b, the spatial linkage ABCD (Figure 2a) uses only a single adjustable screw device GFE (that allows height adjustment of the spherical joint D, depending on the climatic features), and its swing bar 3 has a constant length.
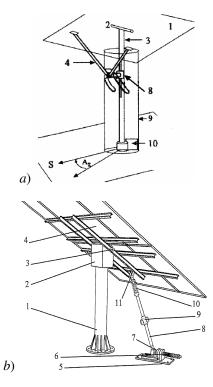

a)

b)

Fig. 1. *a*) *Greek patented solar bi-axial tracking system with a single actuator* [4]; *b*) *Spanish patented solar bi-axial tracking system with a single actuator* [5]
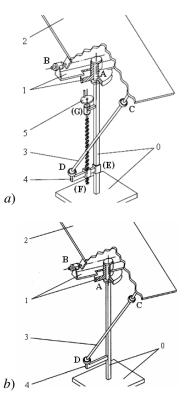

a)

b)

Fig. 2. *a*) *An adjustable variant* [3]; *b*) *A new non-adjustable variant for a bi-axial azimuth tracker driven by a single actuator*

The kinematical synthesis of the adjustable linkage in Figure 2a led, in Braşov's climatic conditions, to the optimal dimensional correlations in Table 1 [3]; according to Figure 3, the notations in Table 1 have the following meanings: $H = h/l_0$, $R = r/l_0$, $L = l/l_0$, α^*_m and α^*_M = minimum and maximum value, respectively, of the considered PV platform altitude, ψ^*_m and ψ^*_M = minimum and maximum value, respectively, of the considered PV platform azimuth [3].

Table 1

Optimum values for the adjustable linkage dimensions during the equinox and the two solstices (see Figure 3) [3]

i	Summer solstice	Equinox	Winter solstice
α^*_M	63°	45.5°	28.5°
ψ^*_M	0°	0°	0°
α^*_m	31°	27.5°	20°
ψ^*_m	90°	90°	56°
H_i	**2.2**	**3.8**	**4.7**
R		**3.4**	
L		**2.02**	

The numerical simulations, based on data in Table 1 [3] (see also Figure 3), highlight that the linkage adjustment (Figure 2a) has a relatively small energetic effect.

That is the reason why this paper continues the research work of the previous paper [3] and proposes a non-adjustable variant of the tracking linkage (see Figure 2b) whose optimal dimensional correlation will be further determined for Braşov's climatic conditions, by means of numerical simulations.

2. Modelling of the Non-Adjustable Tracking Linkage

Knowing that, for Braşov's climatic conditions, the energetic effect of the linkage adjustment (see Figure 2a) is small [3], this paper proposes the non-adjustable variant

illustrated in Figures 2b and 3; the structure of this new variant has been derived from the adjustable linkage (see Figure 2a) by eliminating the screw device EFG and solidifying the elements 4 and 0. In the kinematical modelling that follows, the relative dimensions $R = r/l_0 = 3.4$ and $L = l/l_0 = 2.02$ (see Table 1) [3] are further kept. Using α^*_M as the main adjustable parameter, the optimal relative height $H = h/l_0$ will be determined by numerical simulations.
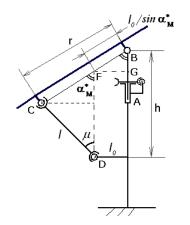

Fig. 3. *Geometrical scheme of the non-adjustable mono-actuator and bi-axial tracking linkage at noon position*

With that end in view, the correlation between $H = h/l_0$ and α^*_M is further determined by means of Figure 3:

$$h = DF + GB = l \cdot \cos \mu + \\ + (r - l_0 / \sin \alpha^*_M) \cos \cdot \alpha^*_M, \qquad (1)$$

$$l / \sin \alpha^*_M = (r - l_0 / \sin \alpha^*_M) / \sin \mu. \qquad (2)$$

From previous relations it results the demanded correlation:

$$H = L \cdot \cos \mu + R \cos \alpha^*_M, \qquad (3)$$

where:

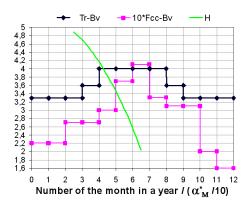$$\mu = \sin^{-1}\left(\frac{R \cdot \sin \alpha^*_M - 1}{L} \right). \qquad (4)$$

Fig. 4. *Variation of the reduced height H vs. angle* α^*_M *, and monthly variations of the turbidity factor* **Tr** *and the clouds' crossing factor* **Fcc***, valid for Braşov area* [2]

In accordance with relation (3), the reduced height variation (*H*) has been illustrated in Figure 4, as a function of angle α^*_M (as well as the monthly variations of the turbidity coefficient *Tr* [6] and the clouds' crossing factor F_{CC}, valid for the climatic conditions in Braşov area [2]).

Subsequently, based on the relation $H = H(\alpha^*_M)$, the optimum constant value of angle α^*_M is determined (i.e. the value corresponding to a maximum amount of direct solar radiation received on the PV module throughout a year). Further on, given the variation of yearly maximum solar altitude $\alpha_M = 22^0 \dots 68^0$ for Braşov area, the first numerical simulations will

$$R_0 = 1367 \cdot [1 + 0.0334 \cdot \cos{(0.9856°\,N - 2.27°)}] , \tag{5'}$$

$$E_{IS} = \sum R_D \, \Delta t, \tag{6}$$

$$E_{RS} = F_{CC} \cdot \sum R_D \, \Delta t, \tag{6'}$$

where: R_D [W/m^2] is the direct solar radiation that falls normally onto the PV platform in ideal conditions (i.e. clear sky); *Tr* is the turbidity factor (see Figure 4); E_{IS} and E_{RS} [Wh/m^2] are energies yielded by the direct solar radiation onto the PV panel

consider, in turn, five constant values of the PV-platform altitude: $\alpha^*_M = 60^0$, 55^0, 45^0, 35^0 and 30^0, respectively (see Figure 4).

3. Numerical Simulations

The accomplishment of numerical simulations consists in determining the direct solar radiation received on the PV platform and assessing its specific energy, under two different circumstances: *a*) ideal (clear) sky and *b*) real (cloudy) sky. These assessments are based on variations in *Tr* and F_{CC} (see Figure 4), valid for Braşov's climatic conditions [2].
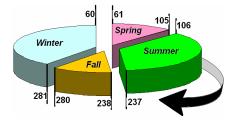

Fig. 5. *Year's seasonal division and seasonal extreme days*

In these numerical simulations, the direct solar radiation, received normally by the PV module, and its specific energy are modelled by means of the following correlations [6]:

$$R_D = R_0 \exp[-T_r / (0.9 + 9.4\sin\alpha)], \tag{5}$$

in ideal (clear sky) and real (cloudy sky) conditions, respectively; F_{CC} is the clouds' crossing factor (see Figure 4) and $\Delta t = 0.5$ [h] is the time interval considered.

The simulations are carried out on representative days: the first, the middle and the last day of each season; with this end in view, the year has been divided into four seasons according to the principal stages of the solar year (Figure 5): spring

equinox (day 80 - 21st March), summer solstice (day 172 - 21st June), autumn equinox (day 266 - 23rd September) and winter solstice (day 355 - 21st December).

The specific energy produced by the direct solar radiation onto the PV platform during a season can be calculated by multiplying the number of each season days and the average energy corresponding to the three simulation days of the season considered. Implicitly, the yearly energy will be the sum of energies corresponding to all four seasons.

For the two yearly solstices and an equinox, the simulation results are illustrated in Figures 6, 7 and 8 respectively, with regard to variations in the following sizes:
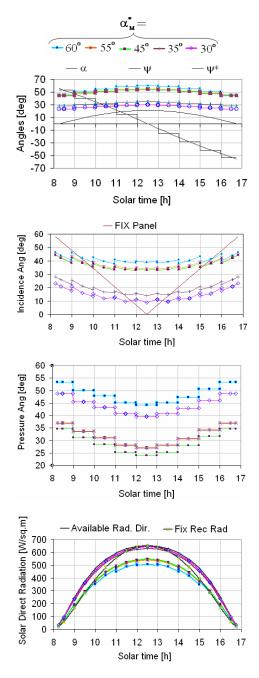
- in the first diagram, a family of curves is illustrated: the solar angles, represented by non-step lines (azimuth ψ and altitude α) and the PV angles, represented by step lines (azimuth ψ^* and five step lines of the altitude α^* corresponding to the five values $\alpha^*_M = 60^0, 55^0, 45^0, 35^0, 30^0$);

- in the second diagram, another family of curves is illustrated: the incidence angles, between sun-ray and PV normal, for a tracked PV platform (in the five cases of α^*_M), as well as for a fixed and tilted PV platform;

- in the third diagram, the variation lines of the pressure angle are plotted (from the joint between PV frame 2 and swing bar 3, see Figure 2b), corresponding to the five values $\alpha^*_M = 60^0, 55^0, 45^0, 35^0, 30^0$. This pressure angle is described by the following relation [3]:

$$\sigma = \cos^{-1}\left(\frac{H}{L}\sin\alpha^* - \frac{1}{L}\cos\alpha^*\cos\psi^*\right); (7)$$

- in the fourth diagram, the variation curves of the direct solar radiation R_D are plotted (in the case of an ideal sky) with respect to: available radiation, radiation that falls normally onto the tracked PV platform (in the five cases of α^*_M), as well as onto a fixed

Fig. 6. *Variations in the main PV-system sizes, during the winter solstice in Braşov, according to $\alpha^*_M = 60^0, 55^0, 45^0, 35^0, 30^0$: solar and PV angles, incidence angles, pressure angles and direct radiation*
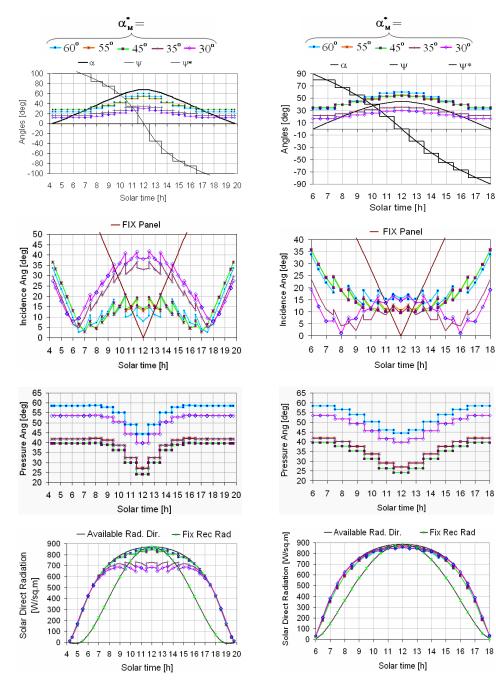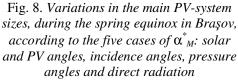
Fig. 7. *Variations in the main PV-system sizes, during the summer solstice in Braşov, according to the five cases of α^*_M: solar and PV angles, incidence angles, pressure angles and direct radiation*

Fig. 8. *Variations in the main PV-system sizes, during the spring equinox in Braşov, according to the five cases of α^*_M: solar and PV angles, incidence angles, pressure angles and direct radiation*
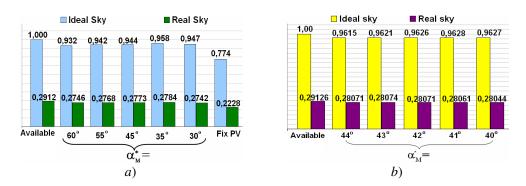
Fig. 9. *Yearly specific energy in Braşov area, given by the direct solar radiation, for both ideal and real sky conditions, in the case of available radiation, radiation that falls normally onto the tracked PV platform, and radiation that falls normally onto a fixed and tilted PV platform, considering: a*) $\alpha^*_M = 60^0, 55^0, 45^0, 35^0, 30^0$ *and b*) $\alpha^*_M = 44^0, 43^0, 42^0, 41^0, 40^0$

and tilted PV platform. The area under each curve represents the daily specific energy [Wh/m^2/day] given by the radiation considered during daylight.

Based on the simulation results, obtained for the 12 representative days in a year, the seasonal and the yearly specific energy were calculated, according to the previous algorithm, in both ideal and real sky conditions. The resulted yearly energy, corresponding to the five cases of α^*_M and the two sky conditions, was graphically systematized in Figure 9a; these results show that the optimal constant value of angle α^*_M ranges between 45^0 and 35^0. Based on these data, the accuracy of α^*_M determination was further increased by considering closer values: $\alpha^*_M = 44^0, 43^0, 42^0, 41^0$, and 40^0. According to these and Figure 9b, the simulation results show that, for Braşov area, in the case of an ideal (clear) sky, the optimal solution should be considered: $\alpha^*_M = 41^0$ and $H = 4.1679$. But, in order to achieve the best amount of energy for Braşov area, in the case of a real (cloudy) sky, the optimal solution is obtained for $\alpha^*_M = 43^0$ and $H = 4.0167$ (see Figure 9b). For this real optimal solution, the variations in the direct solar radiation during

an equinox and the two yearly solstices are shown in Figure 10; it highlights that the PV system has a maximum energetic efficiency and yields a maximum amount of energy during those seasons including the two equinoxes.

4. Conclusions

a) This research starts from the results of a previous paper [3], which shaped a PV adjustable mono-actuator bi-axial azimuth tracker (see Figure 2a) and concluded that the energetic gain of this tracker vs. a non-adjustable one is relatively small;

b) This paper continues the research work of the previous one and proposed a non-adjustable variant of a tracking linkage (see Figure 2b) for which the optimal dimensional correlation was determined, by means of numerical simulations, for the climatic conditions of Braşov area;

c) With this end in view, first the correlation between $H = h/l_0$ and α^*_M was determined. Then, keeping unchanged the reduced dimensions $R = r/l_0 = 3.4$ and $L = l/l_0 = 2.02$ of the adjustable tracking linkage (see Table 1) and using the PV altitude α^*_M as an adjustable but constant parameter, the
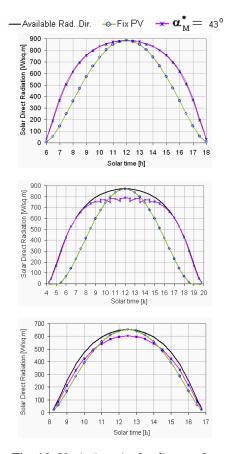
Fig. 10. *Variations in the direct solar radiation during the spring equinox, the summer solstice and the winter solstice, specific to Braşov area, for the tracking linkage with reduced height: H = 4.0167 ($\alpha^*_M = 43^0$) and for a fixed and tilted PV system*

optimal relative height $H = h/l_0$ was established by numerical simulations, in two distinct cases: ideal (clear) sky and real (cloudy) sky;

d) The simulation results highlight the fact that, for Braşov's climatic conditions, the optimal non-adjustable tracking linkage has the following reduced dimensions: $R = 3.4$; $L = 2.02$ and $H = 4.1067$; these reduced lengths allow of a maximum PV platform's elevation angle $\alpha^*_M = 43^0$ at the solar noon;

e) In accordance with Figure 9b, the resulted optimal non-adjustable tracking linkage can yield - in the real climatic conditions of Braşov area - an annual value of about 96% of the available solar energy, which is approximately 26% more energy than a fixed and tilted PV system and about 1% less energy than an adjustable tracking linkage.

References

1. Boyle, G.: *Renewable Energy.* Glasgow. Oxford University Press in Association with the Open University, 2004.

2. Diaconescu, D., et al.: *Clouds Influence on the Solar Radiation for a Mountain Location.* In: Proceedings of the BRAMAT Conference, Braşov, 2009, p. 7-28.

3. Diaconescu, D., et al.: *Synthesis of a bi-Axial Tracking Spatial Linkage with a Single Actuator.* Accepted paper at SYROM Conference, Braşov, October 2009.

4. Fragkiadakis, I.: *Innovative Azimuthal Solar Tracker.* Patent GR 1006107B1, Publication date, 15-10-2009.

5. Jesus, A., et al.: *Solar Tracker with Movement in Two Axes and Actuation in Only One of Them.* Patent WO2008/000867 A1, Publication date, 18-06-2008.

6. Meliss, M.: *Regenerative Energie-quellen Praktikum.* Berlin Heidelberg, Springer, 1997.

7. Messenger, R., Ventre, J.: *Photovoltaic System Engineering.* London. CRC Press, 2000.

8. Visa, I., et al.: *On the Received Direct Solar Radiance of the PV Panel Orientated by Azimuthal Trackers.* In: COMEC - The 2nd International Conf. "Computational Mechanics and Virtual Engineering", Braşov, Romania, October 2007, p. 25-30.